ANTAL KERPELY DOCTORAL SCHOOL OF MATERIALS SCIENCE & TECHNOLOGY

Development of ceramic particle reinforced SAC305 lead-free solder composite material

A Ph.D. dissertation submitted to Antal Kerpely Doctoral School for the degree of

Doctor of Philosophy in the subject of Material Science and Technology

By

Manoj Kumar Pal

Supervisors

Prof. Zoltán Gácsi (Professor)

Dr. Gergely Gréta (Associate Professor)

Head of the Doctoral School

Prof. Zoltán Gácsi

Institute of Metallurgy, Metal Forming, and Nanotechnology

Faculty of Material Science and Engineering

University of Miskolc, Hungary-3515

2021

1. Introduction

New solders are usually Sn-based and the main benchmark for the selection of lead–free solder is that the alloy should be eutectic alloy close. The Sn–Ag–Cu (SAC) is the strongest opponent of Pb-free soldering because it is near to eutectic. NEMI (National Electronics Manufacturing Initiative), Japan Electronics and Information Technology Industries Association (JEITA) suggested an Ag rich composition Sn–3.9Ag–0.6Cu(SAC396), Sn–3.0Ag–0.5Cu(SAC305), and Sn–3.5Ag–0.7Cu(SAC357), and The European Consortium – BRITE-EURAM recommended 95.5wt%Sn–3.8wt%Ag–0.7wt%Cu; Sn–3.8Ag–0.7Cu(SAC387), etc. **[1-2].**

The present dissertation is concentrated on the preparation and characterization of 96.5Sn–3Ag–0.5Cu(SAC305) composite solders containing reinforcement (SiC and SiC–Ni) and the investigation of the microstructural and mechanical properties of composite solder and its joints under the conditions of isothermal aging. The formation of IMCs in lead-free solders with weight variation during the reflow process due to lack of proven data. This research is examined the distribution of the reinforcement in the solder matrix, optimal reflow settings for lead–free solder, and the factor that influences the process are investigated.

2. Literature review

2.1 Composite solder material

There are many different lead-free alloys available nowadays. A solder alloy that is being proposed for the replacement of the traditional Sn–Pb eutectic composition should have its melting point as close as possible to the tin-lead eutectic temperature. The selections are based on a variety of considerations, including toxicity, physical properties (melting temperature, surface tension, wettability, thermal and electrical conductivity), mechanical properties, microstructure characteristics, electrochemical properties (corrosion, oxidation and dross formation, and compatibility with non-clean fluxes), manufacturability, cost, and availability **[3-5].** The preference is given to the Sn–Ag–Cu (SAC) alloy family, followed by alloys containing, silver, copper, bismuth, antimony, indium, zinc, and aluminum.

various researchers have used the ceramics reinforcements in the lead–free solder matrix and prepared the different types of solder composites. Ceramic reinforcements have some favorable properties (ex. chemical stability, abrasion and wear resistance, high strength, hardness, high

melting point (thus high-temperature capability), low density) which makes a promising candidate for the reinforcements. Apart from this, they have poor wetting behavior due to the brittle nature, high hardness, resistance to creep, and high strength, conventional machining methods are difficult to perform because of cracks, brittle fractures, and edge chipping.

2.2 Type of reinforcements

Carbon–based materials, Metal oxide, carbide, and nonmetallic elements are non–reactive reinforcements because they do not react with the solder matrix during the aging and reflow process, and they do not coarsen during their service life. However, such types of reinforcements can not be wetted by the molten solder, during the reflow process generally reveals that they are expelled from the molten solder **[6-7].**

SiC is used because of its low cost and the wide range of sizes and grades available. The addition of SiC increases Young's modulus and tensile strength of the composite materials and it is also increased in wear resistance **[8].** Aqeeli et al. **[8]** reported that SiC can help transfer the shear load at the matrix/reinforcement interface, strengthen the matrix and at the same time retain some ductility. However, while the yield and ultimate strength of the matrix increase with increasing concentration of ceramic particles, the ductility of the composites deteriorate significantly at higher concentrations. SiC has the self-organized dispersive systems property and it can help to formation of the heterogeneous nucleation, thereby distributing stress homogeneously in the solder joints **[9]**. The addition of SiC particles can also improve the sinterability of processed powders. Woo and Zhang **[10]** investigated the SiC-reinforced Al–7Si–0.4Mg composite powders and an increase in the sintering rate of the composite powder was reported due to the increased diffusion rate.

2.3 Mechanical mixing method (Powder metallurgy)

Powder metallurgy (PM) is the most popular manufacturing process. In general, Metal powders are used in the PM process with the specific characteristics of size and shape and then changes it into strong, accurate, and high–performance finished products. There are three main steps to this approach, mixing, compressing, and sintering.

PM technique can be used to produce porous metals, oxide dispersion alloys, ceramic–metal composites, and cemented carbides. The powder metallurgy technique is popular because all processes can be performed in the solid-state and microstructural damage caused by elevated temperatures can be avoided.

2.4 Materials

2.4.1 Solder Matrix Material

Sn–3.0Ag–0.5Cu has superior mechanical properties compared to the other lead-free solders and particularly conventional eutectic Sn–Pb, Therefore, commercial lead-free solder alloy, Sn–3.0Ag–0.5Cu (SAC305) was selected as a matrix material.

2.4.2 Reinforcement Materials

In comparison to other ceramic reinforcing particles, SiC is also a typical ceramic material with excellent chemical stability, low density (3.21 g/cm^3), and high melting temperature (2,730 ºC); it also exhibits good mechanical properties. Additionally, it has also high electrical and thermal conductivity; so for this reason, SiC a potential reinforcement for composite solders without affecting significantly their performance. SiC is supported to form self-organized dispersive systems that can help to formation of the heterogeneous nucleation so that stress can be distributed homogeneously in the solder joints. SiC particles were found to provide additional nucleation places for the formation of the primary β–Sn phase and Ag_3Sn IMCS. **Table 2.1** shows the advantages of SiC ceramic reinforcement.

Table 2.1 Advantages of the SiC ceramic reinforcement

Reinforcement	***Advantages***	**Reference**
SiC	• Low cost and a wide range of sizes and grades available. • It increases Young's modulus, tensile, and wear resistance. • It can be helped the transfer the shear load at the matrix/reinforcement interface, • Strengthen the matrix and at the same time retain some ductility. • It has a self-organized dispersive systems property. • It can help to formation of the heterogeneous nucleation. • It can improve the sinterability of processed powders.	**[8]** **[9]**

2.5 Main problems in the composite solders studied

2.5.1 Distribution of reinforcements in a solder matrix

Generally, the reinforcements are found at the grain boundaries of solder alloys and enhance the mechanical properties of the solder and joint. However, the addition of excessive reinforcement is probably to accumulate and agglomerated in the solder matrices, which can reduce the mechanical

strength of composite solders. Therefore, the reinforcement must be homogeneously distributed in the matrix during the mixing process.

However, it is practically difficult to make a composite solder with homogeneously distributed reinforcements. The mixtures (solder powder and reinforcement particles) are milled for a long period and agglomeration is formed in the composite solder matrices. Various researchers have been successfully fabricated a composite solder with a uniform distribution of reinforcement particles **[12-13].**

2.5.2 Poor wettability

Wettability tends to spread the liquid on a solid substrate and is generally considered by the contact angle. A liquid that spreads on a substrate and does not react by the substrate material is called non-reactive wetting, while the wetting process affected by the reaction between the spreading liquid and the substrate is called reactive wetting **[14]**. The reactive wetting process is influenced by a few more factors, such as soldering temperature, flux, the addition of impurities, etc. However, the correct mechanism which can control the kinetics of wetting is very difficult to predict because reactive wetting is influenced by a lot of the factors, such as interfacial reactions, chemical reaction, diffusion of components, dissolution of the substrate, etc.

(a) ***Surface roughness:*** The rough surface can create the new surface area for the solidified liquid. The new surface area is given by the rough surface and it increases the surface energy. Rough surfaces create a metastable state of equilibrium for the joints and it provides multiple contact angles **[14].**

(b) ***Flux:*** Flux is to overcome the oxidation in the solidification process. The reduction of the oxide layer can obtain the real wetting on the solid substrate and it can change the interfacial properties of the solder joint. It can also protect from re-oxidation and directly affect the surface tension of the solidified solder in the direction of solder spreading **[15]**.

(c) ***Temperature:*** Oxidation behavior, reaction rate, surface tension, and viscosity are influenced by temperature. It is a general phenomenon that the viscosity and surface tension of a liquid decrease with increasing temperature. Therefore, wettability in all systems should improve with increasing temperature **[16]**.

2.6. Knowledge gap

Just a few studies investigated the distribution of the reinforcement particles, optimum composition, and connection between the reinforcement matrix particles. There is a gap in understanding the effect of the connection between the reinforcement and matrix particles. The knowledge is also missing in the systematic qualitative examination of average neighboring particles distance and morphological mosaic analysis of the ceramic reinforcement in the solder matrix.

In addition to this, IMCs layer growth was confirmed with various reflow, aging time, and temperature. The development of the IMCs layer is due to the higher diffusion of the Cu atoms. However, some literature is provided that the growth of the IMCs layers is surpassed with an increase in temperature. There is a need to clarify the behavior of the IMCs layer of the Different time and temperature under reflow and aging condition.

2.7. Scientific goals

Based on these, the present dissertation is emphasized on the preparation and characterization of Sn–3.0Ag–0.5Cu (SAC305) composite solder with various content (0.5, and 1.5 wt. %) of SiC and Ni–coated SiC reinforcements and the examination of physical, microstructural and hardness of a lead-free solder Sn–3.0Ag–0.5Cu. After careful literature review and finding of the knowledge gap, the following scientific aims have been defined:

(1) Identify the optimum composition of the reinforcement in the solder matrix.

(2) Investigate the relative contact perimeter between the reinforcement and lead–free solder particles.

(3) To investigate the average neighboring particle distance and morphological mosaic analysis of the ceramic reinforcement in the solder matrix.

(4) Observe the change in the thickness of the IMCs layer at the Cu–Sn interface and establish the relation between the growth thickness, time, and temperature under reflow and aging condition.

(5) How does the SiC and nickel-coated SiC reinforcements affect the microstructural evolution?

(6) How does the SiC affect the wettability and how does the nickel coating change this?

(7) What effect does increasing the amount of SiC have on wettability and hardness as well as on microstructure?

(8) What changes occur in the microstructure as a result of aging in the case of the composites?

(9) Does nickel coating matter for aging?

(10) What kind of processes takes place during reflow and aging?

(11) How does the thickness of the IMC layer change as a function of time and temperature during reflow and aging?

3. Experimental procedures

The SAC305 powder is blended with SiC and SiC(Ni) powders at various weight fractions. The composite lead–free solders from here on would be marked as SAC–*x%*SiC(Ni), where *x* stands for 0, 0.5, 1, and 1.5wt% for SiC and SiC(Ni). The SAC305 powder and reinforcements (SiC and SiC–Ni) powder particles were pre-weighed and put in a milling jar. They are mixed to achieve homogenization in a planetary ball mill for 1 hour. The rotational speed of the milling process was 200rpm and the ball to powder ratio is 10:1 (BPR). The steel balls used in this process were 3mm in diameter. Ethanol was used as milling media (40 ml). This powder is then compacted under a pressure of 200MPa in a cylindrical die of 15mm diameter. Oil lubricant was used to make the ejection and densification of the post process sample smoother. Following the compaction, the substrate was sintered in a furnace for 3 hours at 200°C under Ar inert gas environment.

To perform the reflow and thermal aging test, a cylindrical sample (3:3 mm in diameter and height) containing two different reinforcements with different compositions were soldered on the Cu substrate. These two types of composite solders were SAC/SiC and SAC/SiC(Ni). The weight of the powder and the compaction pressure was 0.1g and 200MPa. (SAC305)100–*x*(SiC) solder powder was uniaxially compacted in a die (cold pressing at room temperature) to form a cylindrical bar of 3 mm in diameter. The base/substrate was a square copper plate (15 × 15mm) was grinded from sandpaper to achieve a smooth surface for the measurement of contact angle (θ), spread factor (S_f), and spread ratio (S_r) of the solder, 2mm thick copper sheet. Acetone was used to clean and polish the copper plate. A small amount (0.02g) of activated rosin (RA) flux was used on the surface of the sample and in between the solder sample and the Cu substrate.

The solder sample was put on the center of the copper substrate and then the reflow process was conducted. Then, the samples were put in the furnace for melting. it is proven that 1%SiC composition is optimal as compared to other weight percentages (0, 0.5, 1, and 1.5). SAC305/1%SiC is melted at various reflow temperature (240°C, 260°C, 280°C, and 300°C) at different time (30, 60, 90, & 120min.). When performing the thermal aging test, the thermal aging

temperature was set to 140℃, 150℃, 160℃, and 170℃, while the thermal aging times were 0, 25, 50, 75, and 100h.

4. Results and discussion

1.1. Porosity analysis

In addition, the pores that are initially trapped between the particles are reduced during sintering. The porosity reduction during sintering where the pores between the grain boundaries are reduced, resulting in a denser sintered material. These initial large pores become spherical and smaller after sintering. Hence, after a series of careful trial and error run of experiments, the reinforcement composition was limited to 1wt% of both SiC or SiC(Ni) particles.

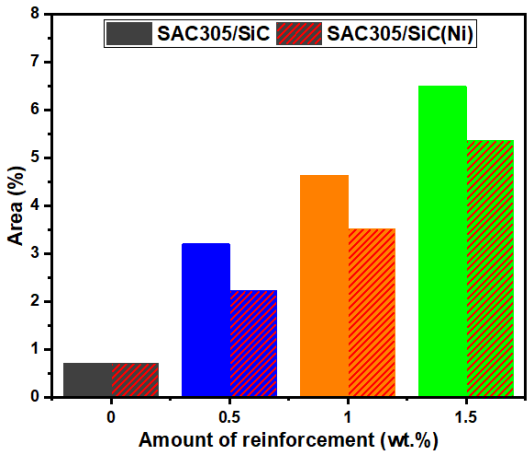

Figure4.1. Porosity analysis of the SAC305 solder composite with the addition of SiC and SiC(Ni)

In the present work, **Figure 4.1** which has 1.5wt%SiC(Ni) reinforcement in SAC305 solder showed the highest ratio of porosity. All other samples show pores and agglomerates of SiC(Ni) particles in between the SAC305 matrix. There is no complete bond between these agglomerates and matrix particles. The percentage of pores in composite increase with an increase in the amount of reinforcements and monolithic lead-free solder is showing the least amount of agglomerates and porosity and 1.5wt.% reinforced SAC305 solder composite showing the highest amount of agglomerates and porosity.

1.2. Compressive strength of the PM solder composite

The compressive strength of SiC and Ni–coated SiC reinforced lead-free solder composite are shown in **Figure 4.2** The increase in reinforcement content increased the strength of the solder composite under compression. The maximum value for SiC and Ni–coated SiC addition was obtained at 1.0wt.% but beyond this, the compressive strength decreased again. The average compressive strength for monolithic SAC305 solder was 34.21MPa while for 1wt% reinforced composite the compressive strength was 42.75MPa for SiC and 45.29MPa for Ni–coated SiC.

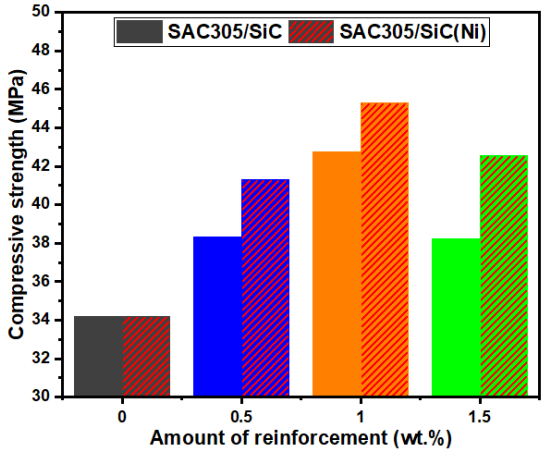

Figure 4.2. Compressive strength of the SAC305 lead–free solder composite with the addition of SiC and SiC(Ni)

Strength is increased due to the addition of ceramic particles because ceramic particles have a higher hardness. In general, the strength of metal matrix composites increases due to the decrease in elongation **[13]**. However, the strength is still higher than the monolithic sample. For a 1% added reinforcement sample, the strength decreased compared to 1.5% by weight because of the presumed increased porosity.

1.3. Relative contact perimeter (RCP) of reinforcement and matrix

Contact perimeter is defined as a contact surface between metallic solder and ceramic reinforcement particles. In **Figure 4.3(a),** the black line indicated the non-contact perimeter, and the rest of the portion is the contact perimeter. Following these analyses carried out for all the samples, the relative contact perimeter follows from following Eq. (4.1).

$$RCP = \frac{P_c}{P_c + P_{nc}} \cdot 100 \qquad Eq.(4.1)$$

Where, RCP is relative contact perimeter, P_c (µm), and P_{nc} (µm) are contact and non-contact perimeter respectively. **Figure 4.3 (b–c)** shows the SEM micrograph of lead–free solder composite with contact and non-contact interfaces between the matrix and reinforcement.

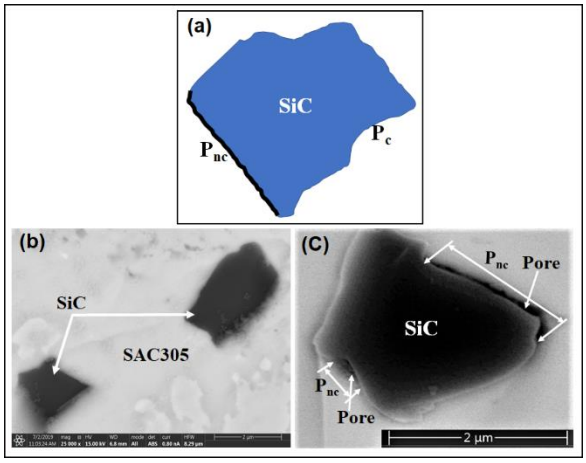

Figure 4.1. (a) Schematic diagram of contact and non–contact perimeter analysis (b) SEM image of SAC305/SiC composite solder (c) SEM micrograph of SAC305 solder composite with contact and non–contact interface

During this study, Ni surface coating was applied on SiC to overcome the weak bonding between lead-free solder and SiC particles. Silicon carbide consists of two types of atoms, the first is silicon atoms and the second is tetrahedral carbon atoms which have strong bonds in the crystal structure. Silicon carbide is a ceramic material with a covalent bond and has stable chemical properties. Ni is a metallic bonded material and it has good wetting characteristics with Sn-based solder because SAC solder has also metallic bonding. In these solder composites, SiC(Ni) is reacted with the SAC305 solder and forms a strong metallic–metallic bond at the interface between reinforcement and solder matrix **[17]**.

The result of **Figure 4.4** shows that the SiC content decreases the contact between the particles and Ni appears at the appropriate position. It is presumed that the Ni particles promotes the RCP of SiC in the solder matrix and avoids direct contact between two or more SiC particles due to metallic bonding. Therefore, micropore formation and agglomeration are significantly reduced. The highest RCP was measured in SiC(Ni) reinforced samples (1.5wt%), while the lowest is in the case of 0.5wt% SiC reinforcement. It is also observed that with the addition of Ni–coated silicon carbide, the relative contact perimeter of composite solders increased drastically.

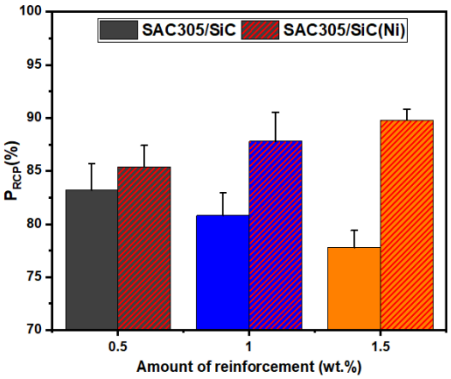

Figure 4.2. Relative contact perimeter of SAC305 lead–free solder composite with the addition of SiC and SiC(Ni)

1.4. Average neighboring particles distance

The average neighbor's particle distance, d_{mn}, is defined as the distance between the centers of gravity between neighboring particles in a matrix. **Figure 4.5 (a)** depicts the variation in average neighbor particle distance, d_{mn} between the reinforcement and matrix particles for various weight fractions. For instance, if the neighbor's particle distance technique is applied to a composite system in which the particles are bunched together in gatherings of at least two, the subsequent closest neighbor's distance tends to the particle diameter, erroneously indicating best clustering, if the second, third, fourth, and so on neighbor's distances are considered **[18]**.

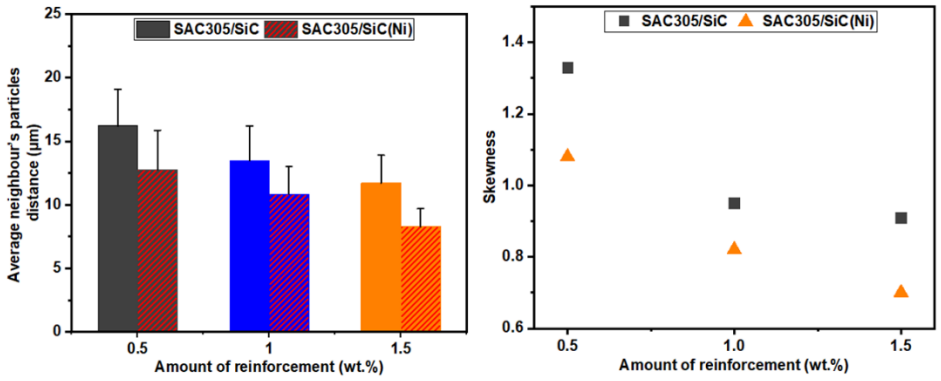

Figure4.3. (a) Average neighbor's particle distance of SAC305 solder composites with the addition of SiC and SiC(Ni) (b) Skewness of SAC305 solder composites

Skewness diagram reveals that the overall shape of the N_q distribution varies significantly with the degree of clustering. An increase in the amount of reinforcement particle clusters has skewed the N_q distribution further. Skewness (β) indicates the degree of asymmetry in the statistical distribution, which is represented by the Eq. (4.2) below **[18].**

$$\beta = {(q)}/{[(q-1)(q-2)]} \sum \left[{\left(N_{qi} - N_q^{mean}\right)}/{(\sigma)} \right]^3 \qquad Eq.(4.2)$$

Where, β = Skewness

q = Total number of quadrats studied, N_{qi} = Number of SiC or SiC(Ni) particles in the i^{th} quadrat (i = 1,2,..,q), N_q^{mean} = Mean number of SiC or SiC(Ni) particles per quadrat, and σ = Standard deviation of the N_q distribution

Figure 4.5(b) shows a variation in β with the varying weight fraction of SiC and SiC(Ni). The skewness ranges between 1.3 to 0.91 for SAC305/SiC composite and between 1.08 to 0.7 for SAC305/SiC(Ni) composite. We see the skewness for SAC305/SiC(Ni) is much broader compared to SAC305/SiC composite solder, which is in agreement with the dissemination of reinforcement particles in lead–free solder. In both reinforcements, it is small changes in skewness i.e. impact of Ni coated SiC is more than SiC.

1.5. IMCs layer thickness at solder/Cu interface

In the case of SAC305 composite solder, the IMC containing Ni was formed at the interface. The Cu atom was joined with the Ni when the solder was melted after reinforcement of SiC(Ni) and the Ni particle absorbed some of the Cu and formed (Ni,Cu)6Sn5 IMC to the interface of the substrate. The diffusion driving force of Cu atoms in the $(Ni,Cu)_6Sn_5$ phase was higher than in the Cu_6Sn_5 phase, and the diffusion pathway of Cu atoms from the Cu substrate was obstructed by the diffusion mechanism **[19-20]**. Therefore, the number of Cu atoms was reduced and the growth rate of $(Ni,Cu)_6Sn_5$ decreased. When the number of reinforcement increases in the solder alloy, more Ni atoms diffused onto the solder surface of the liquid SAC305 and then reacted with Sn and Cu to form the $(Ni,Cu)_6Sn_5$ phase, which affected the growth of IMC. The average thickness (x_t) was calculated by the total area (A) of the individual IMC divided by the total length (L) of the layer, as shown in **Eq. (4.3)**:

$$x_t = \frac{A}{L} \qquad Eq.(4.3)$$

Where, x_t = Average thickness (μm), A = Total area of the individual IMCs (μm^2), and L = Total length of the IMCs layer (μm)

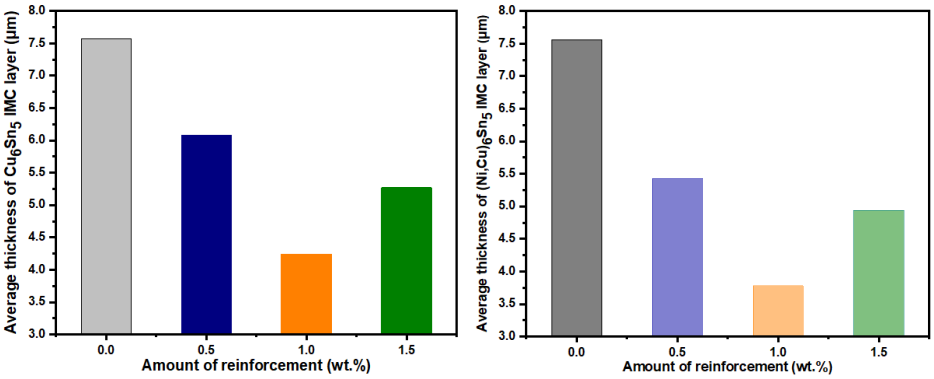

Figure 4.4. Variation of Cu_6Sn_5 and $(Ni,Cu)_6Sn_5$ layer thickness at SAC305/Cu interface

In the monolithic solder, the almost intermittent IMC morphology became smaller in size after the addition of different amounts of SiC and Ni–coated SiC particles. However, the almost intermittent IMC structures became thin and continuous after reinforcing particles were added to the SAC305. It was noticed that the minimum thickness of the IMC layer was obtained by the addition of 1% by weight of SiC and Ni–coated SiC particles.

The growth of Cu6Sn5 and Cu3Sn layer thickness on the Cu substrate was suppressed by the addition of different amounts of reinforcement (SiC and Ni–coated SiC) particles in the solder matrix after 100h aging, as shown in **Figure 4.6 and Figure 4.7.** The thickness of the Cu_6Sn_5 and Cu_3Sn IMCs layer was decreased by 43.8% and 39.6% in the SAC/1%SiC; however, $(Ni, Cu)_6Sn_5$ and Cu_3Sn IMCs layer was reduced by 50.06% and 56.19% in the SAC/1%SiC(Ni) composite solder. The outcome shows that the development of the Cu_6Sn_5, $(Ni,Cu)_6Sn_5$ and Cu_3Sn IMC layer on the Sn–Cu interface was suppressed by a small addition of SiC and SiC(Ni) particles.

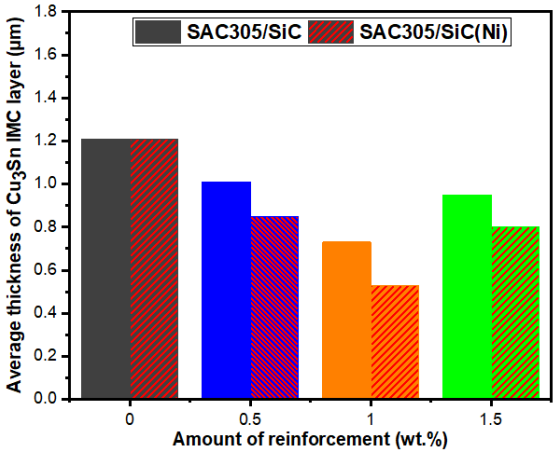

Figure 4.5. Variation of Cu_3Sn thickness at SAC305/Cu interface

1.6. Contact angle (wettability) of composite solder

Adhesion develops from physical (e.g., weak van der Waals) bonds, chemical interactions, and friction from irregular surface **[21]**. The contact angle of the solder on the substrate changed as a function of the amount of reinforcements. The contact angles were calculated by using the following equation **Eq. (4.4) [22]**,

$$\sin\theta = \frac{2}{(d/h) + (h/d)} \qquad Eq.(4.4)$$

The variation of contact angles of composite solders was shown in **Figure 4.8**. The largest contact angle was observed of monolithic SAC305 solder. Initially, the contact angle is decreased from 30.87^{o} to 19.80^{o} for 1%SiC and 16.70 for 1%SiC(Ni), however, an increasing trend was seen afterward.

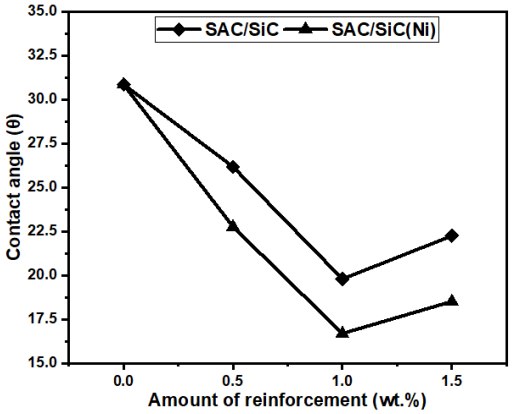

Figure 4.6. Contact angle variation of SAC305 solder with the addition of SiC and SiC(Ni) on Cu substrate

1.7. Spread ratio and spread factor

Spread ratio (S_r) is calculated by measuring the spherical area achieved by the melted solder specimen on the substrate. It is done by measuring the diameter (d) and height (h) of the cooled solder area on the substrate. Spread ratio is taken as the ratio of total plane area wetted by the molten solder on a solid substrate to the plane area of the original solder sample, which is expressed by **Eq. (4.5)** and **Eq. (4.6) [22]**.

$$S_r = \frac{Total\ plane\ area\ wetted\ by\ the\ molten\ solder\ on\ the\ solid\ substrate}{Plane\ area\ of\ the\ original\ spherical\ metal\ sample} \qquad Eq.(4.5)$$

$$S_r = \frac{4d^2/h^2}{[1 + 3d^2/h^2)]^{2/3}} \qquad Eq.(4.6)$$

Where, d is the diameter of the solder sample (mm) and h is the height (mm). Spread factor (S_f) is calculated as the consequence of spread ratio and is given in **Eq. (4.7)** and **Eq. (4.8):**

$$S_f = \frac{Diametre\ of\ the\ original\ solder\ sample\ (d) - \ Height\ of\ the\ spreaded\ molten\ metal\ (h)}{Diametre\ of\ the\ original\ solder\ sample\ (d)} \qquad Eq.(4.7)$$

$$S_f = 1 - \frac{1}{[1 + 3\,d^2/h^2]^{1/3}} \qquad Eq.(4.8)$$

Figure 4.9(a) and **Figure 4.9(b)** shows the variation of spread ratio (S_r) and spread factor (S_f) with the corresponding amount of reinforcements and it was observed that the spread ratio (S_r) and spread factor (S_f) of SAC305 solder increased at 1.0% with an addition of SiC and SiC(Ni). The lowest value obtained for the spread ratio and spread factor is 4.46 and 7.08 for monolithic SAC305 solder, whereas the maximum values were observed to be 6.12 and 7.84 for SAC305/1.0%SiC and 6.88 and 8.08 for SAC305/1.0%SiC(Ni) respectively. The higher amount of reinforcements interrupted the flow of the solder because it is increased the melt viscosity and decrease the spreading of the solders on the substrate **[23-24].**

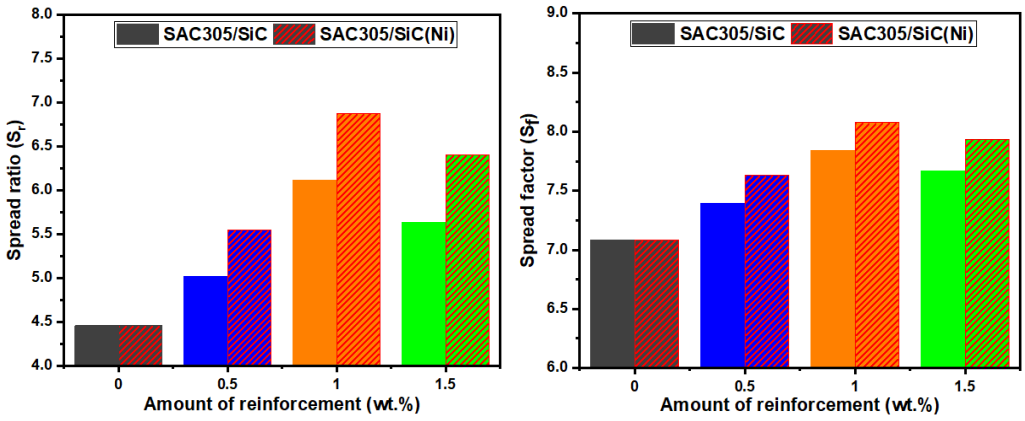

Figure 4.7. Spread ratio and spread factor trend of SAC305 solder composites with the addition of SiC and SiC(Ni)

1.8. Interfacial reactions between Sn–Ag–Cu solder and Cu substrate

SAC305/1%SiC composite solder is selected for examination of the thickness of the Cu_6Sn_5 and Cu_3Sn at the different aged conditions and different times. Generally, Cu_6Sn_5 and Cu_3Sn layers are formed in the Sn–based solder alloys at the Cu–Sn interface, and the thickness of these two layers are increased with increasing aging time. The thickness of the IMCs layer developed at the Cu–Sn interface was examined quantitatively as a function of aging time. The IMC thickness as a function of time can be expressed by the Arrhenius **Eq. (4.9)**:

$$x_t = x_0 + Dt^n \qquad Eq.(4.9)$$

Where, x_t = IMC layer thickness at time t (μm), t = aging time (s), x_0 = Initial IMC layer thickness after aging (μm), D =Diffusion coefficient as a function of temperature (μm^2/s), and n = Time exponent.

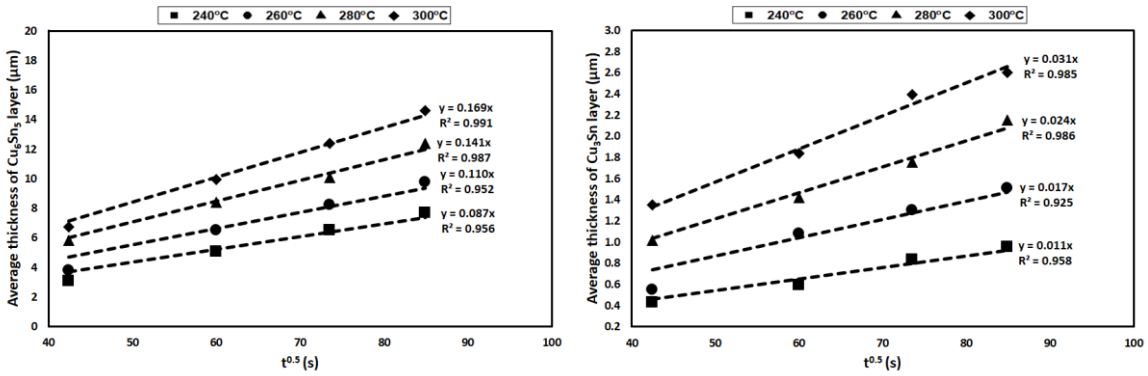

Figure 4.8. Average thickness of Cu_6Sn_5 and Cu_3Sn layer of SAC305/1%SiC composite solder

When plotting the thickness of the intermetallic layer (x_t) against the square root of the aging time ($t^{1/2}$) from **Eq. (4.10)**, the slope of the graph is equal to the square root of the diffusion coefficient ($D^{1/2}$). The diffusion coefficient was determined from a linear regression analysis of x vs $t^{1/2}$, where the slope is $D^{1/2}$.

$$ln(x_t - x_0) = lnD - n.ln(t) \qquad Eq.(4.10)$$

Where, the exponent n is equal to the slope of the $ln(x_t - x_0)\ vs\ ln(t)$ curve. The value of n will be 1/2 when the IMC formation is controlled by the volume diffusion mechanism **[25]**. In this

study, the value *n* under isothermal aging was 0.50. **Figure 4.10 and Figure 4.11** show the IMCs layer thickness (Cu_6Sn_5, and Cu_3Sn) are developed on the Cu–Sn interface at different time and temperatures in reflow and aging process. The thickness of the IMCs layers is increased with an increase of reflow time and temperature.

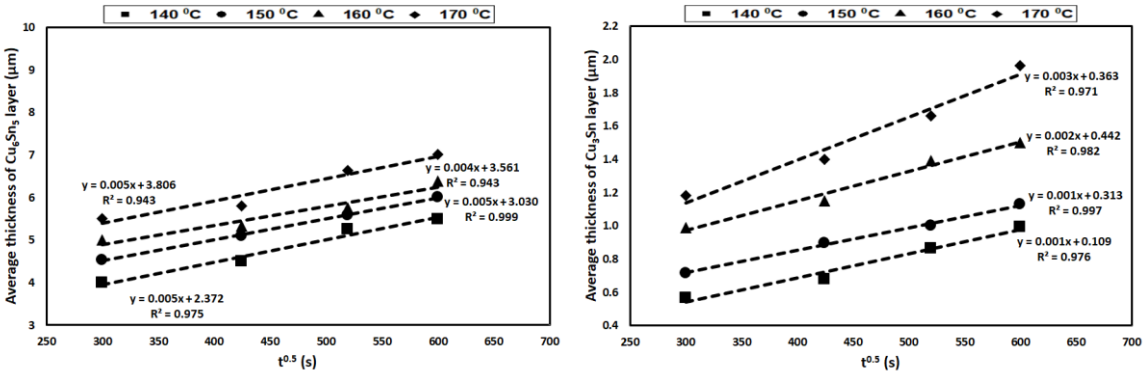

Figure 4.9. Average thickness of Cu_6Sn_5 and Cu_3Sn layer of SAC305/1%SiC composite

The diffusion coefficient of the IMC layers are varied with aging temperature and it is increased with increasing aging temperature. The diffusion coefficient of Cu_3Sn IMC was higher than the Cu_6Sn_5 IMC at aging temperatures of 140 and 170°C, indicating that Cu_3Sn IMC increased rapidly at high temperatures. Cu_3Sn IMC enhanced slowly at low aging temperatures of 140°C.

In the diffusion between lead-free solder and Cu, the development of the IMCs occurs in two ways. First is the interdiffusion and the second is an interfacial reaction. From the Sn–Cu phase diagrams, Sn can react with Cu to form the IMCs layer, while there is no interaction between SiC and Cu because SiC is non-reactive reinforcement and it is gathered in the solder matrix. Chen et al**. [26]** and Chung et al. **[27]** reported that Cu is dominant in the Sn-Cu inter-diffusion process and Cu diffuses towards the Sn with a higher rate because Cu atoms have a lower atomic radius (0.128 nm) than Sn atoms (0.141nm). In the diffusion process, Cu gives sufficient Cu atoms for the origination of the IMCs.

1.9. Calculation of activation energy

The diffusion coefficient at different temperatures was often expressed by Arrhenius **Eq. (4.11)**:

$$D = D_0\, e^{\left(\frac{-Q}{RT}\right)} \qquad Eq.(4.11)$$

Where, D_0 = Temperature-independent diffusion coefficient (m^2/s), Q = Activation energy (kJ/mol), R = Universal gas constant (8.3145 J/K mol), T = Absolute temperature (K)

The activation energy of the intermetallic phase can be determined by (**Eq. 4.11)** and the diffusion coefficient can be indicated as **Eq. (4.12)**:

$$ln(D) = ln(D_0) - \frac{Q}{R}\left(\frac{1}{T}\right) \qquad Eq.(4.12)$$

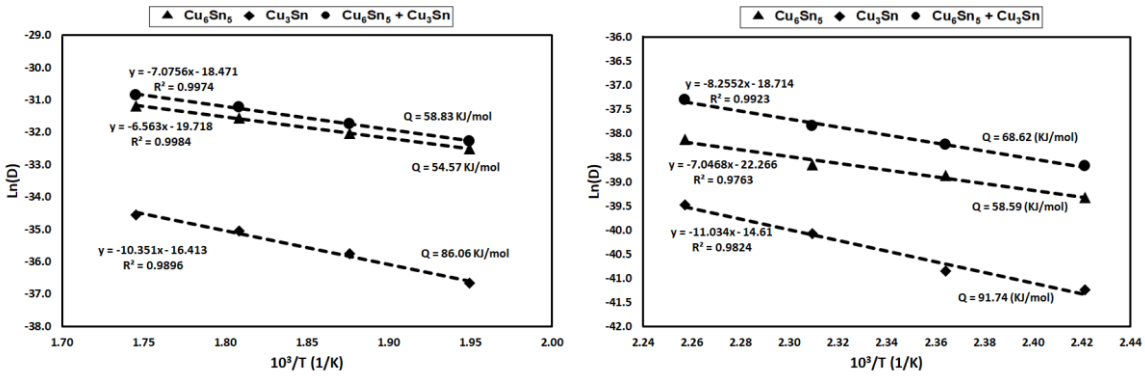

Figure 4.10. Arrhenius plot for the growth of the IMCs layer after the reflow and aging process

Figure 4.12 shows the Arrhenius plots for the growth of the Cu_6Sn_5, Cu_3Sn, and total thickness layers formed at the solder joint after reflow and aging. The activation energies are 54.57, 86.06, and 58.8371kJ/mol for reflow and 91.74, 58.59, and 68.62kJ/mol for aging respectively.

5. Claims

Based on the presented experimental results, the claims below are presented according to the sequence of different phenomena.

Claim (1): In the case of SiC-reinforced solder, composite samples prepared by ball milling and subsequently formed by PM method, experimental data are proved that the use of nickel-coated SiC reinforcement particles promotes homogeneous distribution of reinforcement particles, reduces the porosity area, and provides higher strength.

(1.a) Average neighbour's particle distance are described the agglomeration and dispersion of reinforcement particles in the matrix. The poor dispersion of the particles is due to the agglomeration of the particles in the matrix and may lead to the weakening of the mechanical properties. Skewness diagram revealed that the N_q (number of the reinforcing particles) distribution varies significantly with the reinforcement composition. Average neighbour's

particle distance of both composite solders seen to decrease as the weight fraction of reinforcement increased. The experimental results confirmed that Ni-coated SiC has a lower skewness value and average neighbour's particle distance than the SiC i.e the distribution of Ni-coated SiC particles are more homogeneous than the SiC particles in the SAC305 solder.

(1.b) Ni–coated SiC reinforced composite solder has a lower porosity than SAC305/SiC composites because the reinforcement particles distributed homogeneously. As a result of this homogeneous distribution, the Ni–coated SiC was less clustered, thus a reduced amount of porosity formed around the clusters.

(1.c) According to the lower porosity content, the changes in the compressive strength of the composite solders were observed and the SAC305/SiC(Ni) solder composite has higher compressive strength than the SAC305/SiC.

(1.d) SiC decreases contact angle and increases the spread area because the SiC composites are probably decreasing the surface energy of the copper substrate. The application of the Ni coating further reinforces this tendency because Ni has a higher adsorption capacity and it is reduced the surface energy and growth velocity of the IMC. Added Ni-coated SiC particles accumulated at the interface between the molten solder and the flux during soldering; thereby lowering the interfacial surface energy.

Claim (2): Relative contact perimeter (RCP) is defined as a contact surface between metallic solder and ceramic reinforcement particles and this is a new parameter - which is not been applied in the literature. The increment of RCP in the SAC305 solder composites was observed experimentally measuring the change of reinforcement content. Experimental results are proven that Ni-coated SiC particles are improved the relative contact perimeter. This is an effective value to determine the extent of the contact surface, which determines the properties of the composite. The increment of RCP in the SAC305 solder composites was observed experimentally measuring the change of reinforcement content.

(2.a) Experimental results were proven that the RCP was increased in the Ni–coated SiC reinforced samples. Silicon carbide is a ceramic material with a covalent bond and has stable chemical properties. Ni is a metallic bonded material and it has good wetting characteristics with Sn-

based solder because SAC305 solder has also metallic bonding. The SiC(Ni) particles are easily reacted with the SAC305 solder particles and form a strong metallic–metallic bond at the interface.

Claim (3): Thickness of the interfacial IMCs layer between the solder and Cu substrate shows the difference after the addition of SiC and Ni–coated SiC reinforcement to SAC305 solder. It can be used to simulate how the IMC layer changes during reflow and aging under the influence of time and temperature.

(3.a) The thickness of interfacial IMCs between solder and Cu substrate shows an obvious difference after the addition of SiC and Ni-coated SiC in the SAC305 solder. The reduction of the IMCs layer on the Sn-Cu interface was observed experimentally during the reflow process. These reinforcement particles reduce the surface energy and inhibit the growth of IMC layers.

During the reflowing process, the SiC and Ni-coated SiC particles are distributed in the liquid because it does not melt on the Cu surface due to the high melting temperature. The SiC and Ni-coated SiC particles can behave as a barrier to the diffusion of Cu atoms from the substrate. The results are proven that IMCs layer thickness decreased as the amount of SiC and Ni-coated SiC increases in the SAC305 solder.

(3.b) The experimental results are shown that as time (aging and reflow) and temperature increase, the thickness of interfacial IMCs (Cu_6Sn_5 and Cu_3Sn) are both increased. Ceramic particles enhanced the activation energy which reduced the reaction rate as it is well known that lower activation energy indicates a faster reaction rate. Although this phenomenon is also observed in composite solders, the growth rate of interfacial IMCs is inhibited after the addition of SiC and Ni-coated SiC reinforcement. The activation energy of Cu_6Sn_5 was observed to be lower than that of Cu_3Sn. The activation energy of the (Cu_6Sn_5+Cu_3Sn) lies in between Cu_6Sn_5 and Cu_3Sn phases which appears reasonable. I proved that the IMCs layer thickness is dependent on time (reflow and aging) and temperature (reflow and aging). and this method relies on the calculation of activation energies by plotting the diffusion coefficient as the function of temperature (reflow and aging).

References:

[1] Suganuma, Katsuaki. "Advances in lead-free electronics soldering." *Current Opinion in Solid State and Materials Science* 5, no. 1 (2001): 55-64.

[2] Lau, John, Walter Dauksher, Joe Smetana, Rob Horsley, Dongkai Shangguan, Todd Castello, Irv Menis, Dave Love, and Bob Sullivan. "Design for lead-free solder joint reliability of high-density packages." *Soldering & surface mount technology* 16 No. 1 (2004): 12-26.

[3] Shangguan, Dongkai, Achyuta Achari, and Wells Green. "Application of lead-free eutectic Sn-Ag solder in no-clean thick film electronic modules." *IEEE Transactions on Components, Packaging, and Manufacturing Technology: Part B* 17, no. 4 (1994): 603-611.

[4] Shangguan, Dongkai. "Leading the Lead-free transition." *Circuits Assembly, March* (2004).

[5] Vianco, Paul T., and Darrel R. Frear. "Issues in the replacement of lead-bearing solders." *JOM* 45, no. 7 (1993): 14-19.

[6] Liu, Johan, Cristina Andersson, Yulai Gao, and Qijie Zhai. "Recent development of nano-solder paste for electronics interconnect applications." *10th Electronics Packaging Technology Conference*, IEEE, (2008): 84-93.

[7] Chen, Guang, Fengshun Wu, Changqing Liu, Vadim V. Silberschmidt, and Y. C. Chan. "Microstructures and properties of new Sn–Ag–Cu lead-free solder reinforced with Ni-coated graphene nanosheets." *Journal of Alloys and Compounds* 656 (2016): 500-509.

[8] Al-Aqeeli, N., K. Abdullahi, A. S. Hakeem, C. Suryanarayana, T. Laoui, and S. Nouari. "Synthesis, characterisation and mechanical properties of SiC reinforced Al based nanocomposites processed by MA and SPS." *Powder Metallurgy* 56, no. 2 (2013): 149-157.

[9] El-Daly, A. A., M. Abdelhameed, M. Hashish, and A. M. Eid. "Synthesis of Al/SiC nanocomposite and evaluation of its mechanical properties using pulse echo overlap method." *Journal of Alloys and Compounds* 542 (2012): 51-58.

[10] Woo, K. D., and D. L. Zhang. "Fabrication of Al–7wt%Si–0.4 wt% Mg/SiC nanocomposite powders and bulk nanocomposites by high energy ball milling and powder metallurgy." *Current Applied Physics* 4, no. 2-4 (2004): 175-178.

[11] Suryanarayana, Cury. "Mechanical alloying and milling." *Progress in materials science* 46, no. 1-2 (2001): 1-184.

[12] El-Daly, A. A., A. Fawzy, S. F. Mansour, and M. J. Younis. "Novel SiC nanoparticles-containing Sn–1.0Ag–0.5Cu solder with good drop impact performance." *Materials Science and Engineering: A* 578 (2013): 62-71.

[13] Fathian, Zahra, Ali Maleki, and Behzad Niroumand. "Synthesis and characterization of ceramic nanoparticles reinforced lead-free solder." *Ceramics International* 43, no. 6 (2017): 5302-5310.

[14] Kumar, Girish, and K. Narayan Prabhu. "Review of non-reactive and reactive wetting of liquids on surfaces." *Advances in colloid and interface science* 133, no. 2 (2007): 61-89.

[15] Vaynman, S., and M. E. Fine. "Development of fluxes for lead-free solders containing zinc." *Scripta materialia* 41, no. 12 (1999): 1269 –1271.

[16] Bernardin, John D., Issam Mudawar, Christopher B. Walsh, and Elias I. Franses. "Contact angle temperature dependence for water droplets on practical aluminum surfaces." *International journal of heat and mass transfer* 40, no. 5 (1997): 1017-1033.

[17] Pal, Manoj Kumar, Gréta Gergely, Dániel Koncz-Horváth, and Zoltán Gácsi. "Characterization of the interface between ceramics reinforcement and lead-free solder matrix." *Surfaces and Interfaces* (2020): 100576.

[18] Karnezis, P. A., G. Durrant, and B. Cantor. "Characterization of reinforcement distribution in cast Al-alloy/SiCp composites." *Materials Characterization* 40, no. 2 (1998): 97-109.

[19] Nogita, Kazuhiro, and Tetsuro Nishimura. "Nickel-stabilized hexagonal $(Cu,Ni)_6Sn_5$ in Sn–Cu–Ni lead-free solder alloys." *Scripta Materialia* 59, no. 2 (2008): 191-194.

[20] El-Daly, A. A., A. M. El-Taher, and T. R. Dalloul. "Enhanced ductility and mechanical strength of Ni-doped Sn–3.0Ag–0.5Cu lead-free solders." *Materials & Design* 55 (2014): 309-318.

[21] Asthana, Rajiv, and Natalia Sobczak. "Wettability, spreading, and interfacial phenomena in high-temperature coatings." *JOM-e* 52, no. 1 (2000): 1-19.

[22] Humpston, Giles, and David M. Jacobson, eds. *Principles of soldering*. ASM international, 2004.

[23] Gain, Asit Kumar, Yan Cheong Chan, and Winco KC Yung. "Microstructure, thermal analysis and hardness of a Sn–Ag–Cu–1wt% nano-TiO_2 composite solder on flexible ball grid array substrates." *Microelectronics Reliability* 51, no. 5 (2011): 975-984.

[24] Sharma, Ashutosh, B. G. Baek, and Jae Pil Jung. "Influence of La_2O_3 nanoparticle additions on microstructure, wetting, and tensile characteristics of Sn–Ag–Cu alloy." *Materials & Design* 87 (2015): 370-379.

[25] Osamura, K., S. Ochiai, S. Kondo, M. Namatame, and M. Nosaki. "Influence of third elements on growth of Nb_3Sn compounds and on global pinning force." *Journal of materials science* 21, no. 5 (1986): 1509-1516.

[26] Chen, L. D., M. L. Huang, and S. M. Zhou. "Effect of electromigration on intermetallic compound

formation in line-type Cu/Sn/Cu interconnect." *Journal of Alloys and Compounds* 504, no. 2 (2010): 535-541.

[27] Chung, C. Key, Jenq-Gong Duh, and C. R. Kao. "Direct evidence for a Cu-enriched region at the boundary between Cu6Sn5 and Cu3Sn during Cu/Sn reaction." *Scripta Materialia* 63, no. 2 (2010): 258-260.

Author publications

Journal papers

1. **Pal, M. K.**, Gergely, G., Horváth, D. K., & Gácsi, Z, Microstructural investigations and mechanical properties of pure lead-free (Sn–3.0Ag–0.5Cu and Sn–4.0Ag–0.5Cu) solder alloy. **Metallurgical and Materials Engineering**, 24 (1) **(2018)**, 27–36.
2. **Pal, M. K.,** Gergely, G., Horváth, D. K., & Gácsi, Z., influence of ceramic particles on the microstructure and mechanical properties of SAC305 lead-free soldering material, **Arch. Metall. Mater.** 64 (2) **(2019)**, 603–606.
3. Koncz-Horvath, D., Molnar, A., Gergely, G., **Pal, M. K**., & Gacsi, Z., Examination the effect of thermal shock test on SAC solder joints fabricated by THRS and multi-wave soldering techniques. **Resolution and Discovery**, 4(1) **(2019)**, 1–6.
4. **Pal, M. K.**, Gergely, G., Horváth, D. K., & Gácsi, Z., Investigation of the electroless nickel plated SiC particles in SAC305 solder matrix, **Powder metallurgy and metal ceramics**, 58(9–10) **(2020)**, 529–537.
5. **Pal, M. K.,** Gergely, G., Horváth, D. K., & Gácsi, Z., Characterization of the interface between ceramics reinforcement and lead-free solder matrix, **Surfaces and Interfaces**, 20(3) **(2020),** 100576.
6. **Pal, M. K.**, Gergely, G., Horváth, D. K., & Gácsi, Z., Distribution and microstructure analysis of ceramic particles in the lead-free solder matrix, **Crystal Research and Technology**, 55(10) **(2020)**, 2000123**.**
7. **Pal, M. K.**, Gergely, G., Horváth, D. K., & Gácsi, Z., Investigation of microstructure and wetting behavior of Sn-3.0Ag-0.5Cu (SAC305) lead–free solder with additions of 1.0 wt. % SiC on copper substrate, **Intermetallics**,128 **(2021)** 106991.